Nanoclusters in Zeolite

Pascale Armand,* Marie-Louise Saboungi, D. L. Price, L. Iton, Cornelia Cramer,† and M. Grimsditch

Argonne National Laboratory, Argonne, Illinois 60439
(Received 12 December 1996)

Nanoclusters of Se, Rb-Se, and Cs-Se were incorporated in the supercages of Y zeolite. Anomalous x-ray scattering established that the Se clusters take the form of weakly interacting chains with a disordered structure similar to that of amorphous Se, while the Rb-Se and Cs-Se clusters contain Se_2^{2-} Zintl ions as in crystalline and liquid bulk phases. The Raman spectra of the nanoclusters exhibit features found in the bulk disordered phases. [S0031-9007(97)03938-0]

PACS numbers: 61.46.+w, 61.10.Eq

Confined geometry on the nanometer scale produces dramatic effects on the optical, electronic, vibrational, and thermodynamic properties of condensed matter [1]. Recently, a particle-size-dependent reduction of the latent heat of fusion and of the melting point has been experimentally established in Sn particles of 5 to 50 nm dimension [2]. Porous structures such as zeolites, which are about 30%–50% void space after dehydration, provide a mechanism for confining materials in a controlled fashion, leading to a wide range of applications including molecular filters, electronic devices, and nuclear waste storage. In this work, we have formed nanoclusters of Se and semiconducting alkali-selenium compounds inside zeolite cages 1.3 nm wide and investigated the local surroundings of the Se and Rb atoms with anomalous x-ray scattering (AXS). In the past, semiconducting materials such as Se [3–7], Se-S, Se-Te [4], and Rb-Te [7] alloys, and CdS, CdSe, CdTe, ZnS, and PbS compounds [8,9] have been incorporated in zeolites, but a detailed structural picture at the atomic level could not be obtained since the methods used give limited structural information, especially beyond the nearest neighbors. This is a particular problem if, as in the cases studied here, the incorporated material is structurally disordered relative to the zeolite host.

The AXS technique combines site specificity with unambiguous interpretation of pair correlations in real space and is thus extremely powerful for solving the structure of nanoclusters contained as a minority species in a macroscopic host. In this paper we report results of an AXS investigation of Se, RbSe, and CsSe clusters incorporated into the supercages of Nd-exchanged Y zeolite. These semiconductors were chosen for their unusual temperature- and concentration-dependent properties. In contrast to the more traditional semiconductors (e.g., CdSe, CdTe), these materials have not been synthesized in nanocrystalline form. Furthermore, Se, Rb, and Cs have x-ray absorption edges in a favorable energy region for synchrotron x-ray beams.

The aluminosilicate framework of Y zeolite is of the faujasite type [10] and consists of corner sharing AlO_4 and SiO_4 units connected so that well defined cavities and channels are formed. The supercages are 13 Å in diameter and the connecting channels 7 Å across. In the present work the Na^+ counterions were exchanged with Nd^{3+}; the resulting Nd-Y zeolite offers the advantage that all the counterions are located in the sodalite cages and thus do not play any role in the AXS. Se was introduced into the zeolite by vapor diffusion producing a uniformly orange colored powder. Subsequently, part of this powder was inserted into silica containers fitted with frits, and sufficient quantities of alkali metal were added to form ASe ($A =$ Rb, Cs) stoichiometric compounds. The bottom part of the tubes (where the alkali metal resided) was heated to 320 °C to minimize Se desorption from the zeolite. The resulting material was homogeneously brown, and chemical analysis indicated compositions of $Rb_{0.52}Se_{0.48}$ and $Cs_{0.45}Se_{0.55}$.

Transmission electron microscopy (TEM) measurements revealed a uniform cage structure with a periodicity of ~1 nm. There was no sign of external Se particles, while energy-dispersive analysis confirmed the presence of Se in the host crystal. There was evidence of a few small particles extrinsic to the zeolite micropores in the NdY/RbSe and NdY/CsSe samples, but most of the alkali selenide material was incorporated in the zeolite. Neutron powder diffraction measurements showed that (a) the Nd-exchanged zeolite has a typical Y-zeolite structure with Nd^{3+} ions residing in the sodalite cages, (b) the structure of the zeolite host is preserved upon incorporation of the semiconductors, and (c) the incorporated atoms are largely out of registry with the zeolite [11].

The internal structures of the clusters were determined by AXS measurements at the Se and Rb K edges, carried out on the X-7A beam line at NSLS. With this technique, the structure factor associated with a specific element a is determined from the difference of the scattered intensities taken at two x-ray energies, one just below an absorption edge of the element a, and the other a little farther below. The formalism of this technique is described in detail elsewhere [12]. The chosen energies (in keV) were 12.650 and 12.163 near the Se edge, observed at 12.666, and 15.195 and 14.682 near the Rb edge, observed at 15.214. This method makes it possible to distinguish the environments of Rb and Se in the cluster from those of the zeolite atoms.

The real-space correlation function $T_{SeSe}(r)$ for the Se-loaded zeolite is shown in Fig. 1. The first peak can
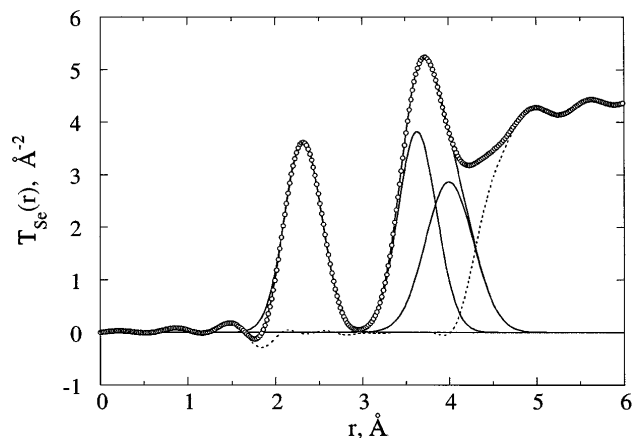
FIG. 1. Se difference pair correlation function for Se in Nd-Y zeolite, with fitted Gaussian peaks.

be fitted with a single Gaussian peak and the second peak, partially resolved from the remaining section of the correlation function, with a pair of unresolved Gaussian peaks. If a peak can be assigned to a unique atom pair (a, j), the average coordination number (CN) $C_n(a, j)$ of j atoms about an a atom can be derived from its area [12]. Comparison with bulk crystalline (c-) and amorphous (a-) Se leads to the assignment of the two peaks at 2.32 and 3.66 Å with Se-Se correlations and the third at 4.00 Å with Se-host atom correlations. The fit for the unresolved second and third peaks is, of course, not unique, but the *position* of the second peak is rather well defined by the leading edge. Comparison of the present results for Se clusters in zeolite with data for the various crystalline [trigonal (t-Se) helical chain structure [13], monoclinic (m-Se) Se_8 ring structure [14], and rhombohedral (r-Se) Se_6 ring structure [15]], glassy (a-Se) [16] and liquid (ℓ-Se) phases [17], grouped in Table I, leads to several important conclusions. First, the nearest-neighbor bond length and coordination number in the Se-loaded zeolite is similar to that in the bulk phases. Second, the second-neighbor bond length is also similar, while its coordination number is significantly lower than in bulk c-Se. It should

be noted that, in spite of the significant difference between the structures of t- and m-Se, the short-range structures are rather similar. The local structure of the two are nearly identical for groups of four atoms on the same chain or ring, and only differ in whether the fifth atom is situated in a trans- or cis-configuration. On this basis, a disordered chain model for ℓ-Se (and by implication for a-Se) was proposed in which trans- and cis-configurations are adopted randomly with statistical weights that depend on temperature [18]. The short-range structure observed here points to a similar disordered chain structure for the Se nanoclusters.

The coordination number for the second shell is 4 ± 1, greater than the value of 2.0 or less expected for isolated chains but lower than the values of 6–7 observed in c- and a-Se. In fact, it is similar to the values found in ℓ-Se— 3.75 at 265 °C, falling to 3.1 at 680 °C [17]. This suggests that the Se nanoclusters consist of a small number of weakly interacting chains. It has been suggested [19] that for faujasites of the kind used here Se forms weakly interacting double chains, which is consistent with our present observation.

Additional support for this conclusion is provided by Raman scattering measurements. In Fig. 2 the spectrum obtained for the Se-loaded zeolite is presented. The spectrum is dominated by one peak around 250 cm^{-1} with a shoulder near 235 cm^{-1} and a broad peak at 190 cm^{-1}. The first peak and shoulder are remarkably similar to those reported by Carroll and Lannin [20] for both a- and ℓ-Se. Lucovsky [21] has pointed out that the variations in trans- and cis-configurations, as well as in the degree of coupling with neighboring chains, should have significant effects on the optical spectra. Both chainlike and ringlike elements should have peaks around 250 cm^{-1}, while strong interactions with neighboring chains should lead to a peak around 235 cm^{-1}, as observed in t-Se. The remaining peaks are similar to those reported in various forms of a-Se [22]. The similarity of the spectrum from the Se-loaded zeolite to that of a-Se, but with a broadening reminiscent of the liquid spectrum, supports the presence of weakly interacting chains. The orange

TABLE I. Short-range structural parameters for Se in zeolite and for various forms of bulk Se; ϕ is the bond angle $[R_2 = 2R_1 \sin(\phi/2)$, where the intra value for R_2 is taken in the crystals and the average value for the other cases]. The values for m-Se are for the α modification; those for β and γ are similar [14].

Form	C_1(Se, Se)	R_1(Å)	C_2(Se, Se)	R_2(Å)	ϕ	Ref.
NdY/Se	2.0 ± 0.3	2.32 ± 0.02	4 ± 1	3.66 ± 0.02	$104° \pm 2°$	This expt.
t-Se: intra	2.0	2.373	2.0	3.716	103.1°	[13]
inter			4.0	3.436		
m-Se: intra	2.0	2.336	2.0	3.72	105.7°	[14]
inter			2.9[a]	3.80[a]		
r-Se: intra	2.0	2.356	2.0	3.64	101.1°	[15]
inter			4.0[a]	3.54[a]		
a-Se	2.0	2.36	7 ± 1	3.74	104.8°	[16]
ℓ-Se(265 °C)	2.0	2.38	3.4	3.75	104°	[17]

[a]Average number of atoms at a distance between 3 and 4 Å, and average distance for those atoms.
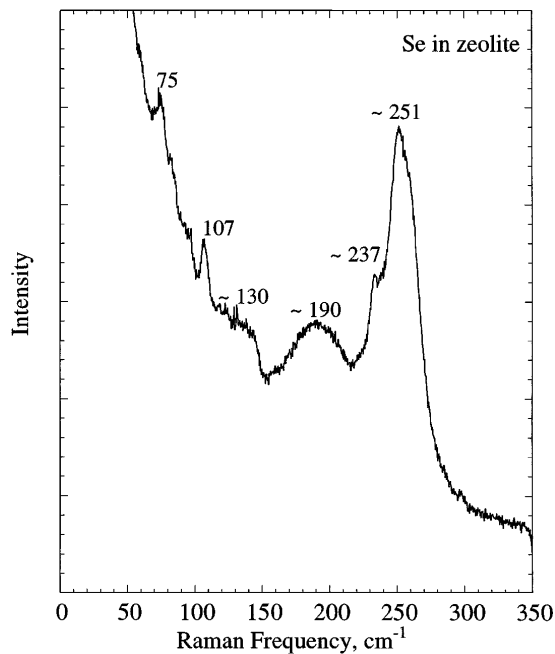
FIG. 2.   Polarized Raman spectrum of Se in Nd-Y zeolite.

FIG. 3.   Se and Rb difference pair correlation functions for RbSe in Nd-Y zeolite, with fitted Gaussian peaks.

color of the Se-loaded zeolite is also consistent with a structural similarity to bulk a-Se.

For the Rb-Se loaded zeolite, chemical analysis confirmed the formation of $Rb_{0.52}Se_{0.48}$. According to the Zintl-Klemm rule in which electron transfer from the alkali moves the chemical properties of the Group-VI atom into line with those of Group VII, Se_2^{2-} polyanions will be present in the crystal and by analogy with KTe [23] are likely to persist in the disordered state, giving a Se coordination number of one. In the case of Cs-Se, the chemical analysis yielded $Cs_{0.45}Se_{0.55}$ which according to the phase diagram will consist of a mixture of CsSe and Cs_2Se_3, and so both charged Se_2^{2-} dimers and Se_3^{2-} trimers are expected to be present, yielding an average coordination number of Se higher than one and less than two.

The real-space correlation functions for the Rb-Se loaded zeolite at the Se and Rb K edges are shown in Fig. 3, with the first four peaks fitted by Gaussians. It is seen immediately that the peak at 2.42 Å appears only in $T_{Se}(r)$ and not in $T_{Rb}(r)$, indicating that it is due to Se-Se nearest neighbors. In c-RbSe [24], the shortest interatomic distance is between a pair of Se atoms, 2.468 Å. Similarly, in ℓ-CsSe [25], the first shell in the pair correlation function results from a pair of Se atoms separated by 2.37 Å. Se_2^{2-} Zintl ions are evidently present also in the RbSe clusters formed in the zeolite supercages. The second peak in $T_{Se}(r)$—the first in $T_{Rb}(r)$—is a broad structure between 3 and 4 Å, partially resolved from the high-r part of the pair correlation function. The Gaussian fits to these peaks give an unresolved doublet at 3.46 and 3.80 Å for $T_{Se}(r)$ and an unresolved doublet at 3.47 and 3.71 Å for $T_{Rb}(r)$. In c-RbSe, each Se atom is surrounded by the other Se atom in the Zintl ion at 2.468 Å, 3 Rb atoms at 3.338 Å, 3 more Rb at 3.620 Å, and 1 Se atom at
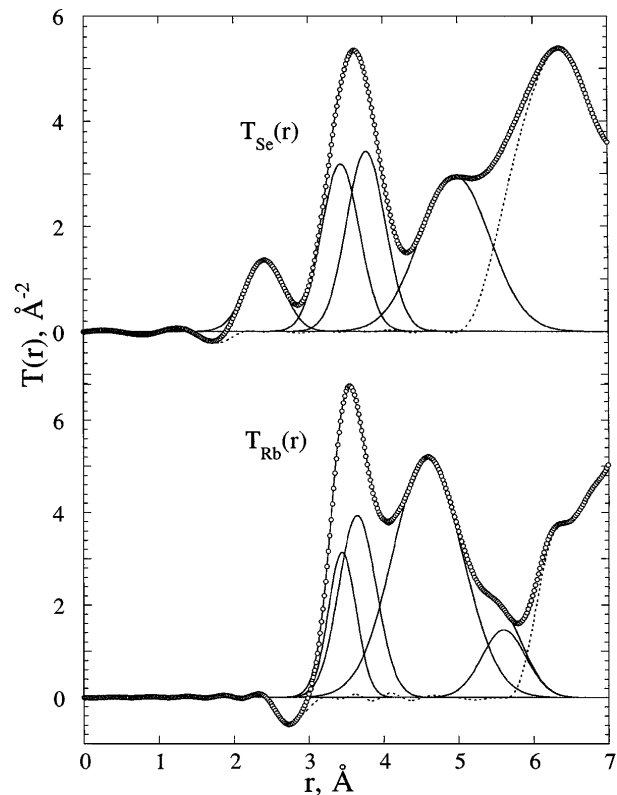
3.734 Å, while each Rb atom is surrounded by 3 Se atoms at 3.338 Å and 3 more Se at 3.620 Å. In bulk ℓ-CsSe, the first Cs-Se distance appears at $\sim$3.46 Å. Thus, it is reasonable to associate the first peak of the doublet in both functions with the Rb-Se nearest-neighbor distance, and the second with subsequent correlations involving both Rb and Se atoms for the Se edge function and Se atoms for the Rb edge function. Parameters derived for the RbSe-loaded zeolite and CsSe-loaded zeolite are given in Table II along with those for c-RbSe and ℓ-CsSe. It is evident that the RbSe and CsSe form clusters in the zeolite that mimic the structure of the bulk compounds.

This conclusion is again reinforced by Raman scattering results. Figure 4 compares the spectrum obtained from the CsSe-loaded zeolite with those from c-CsSe and ℓ-CsSe. The crystal spectrum is characterized by two peaks at 252 and 272 cm^{-1}, the lower of which is ascribed on the basis of *ab initio* quantum chemical calculations [24] to stretching vibrations of the Se_2^{2-} Zintl ions and the higher to vibrational modes involving both cations and anions. The liquid spectrum has a single broad, asymmetric peak around 260 cm^{-1}. The CsSe-loaded zeolite shows a relatively sharp peak around 255 cm^{-1} with a high broad distribution on its low-energy side and a small shoulder on the high-energy side. It is reasonable to associate the 255 cm^{-1} peak with stretching vibrations of the Se_2^{2-} and Se_3^{2-} ions and the broad features on either side with modes involving both cations and anions.

TABLE II. Coordination numbers and bond distances for ASe (A = Rb, Cs) clusters in zeolite, c-RbSe, and ℓ-CsSe.

Form	a[a]	C_1(Se, Se)	R_1(Å)	$C_2(A$, Se)	R_2(Å)	$C_3(a, j)$[b]	R_3(Å)	Ref.
NdY/RbSe	Se	1.1 ± 0.1	2.42 ± 0.02	3.4 ± 0.5	3.46 ± 0.02	3.4 ± 0.5	3.80 ± 0.02	This work
NdY/RbSe	Rb	$\cdots$	$\cdots$	3.1 ± 0.8	3.47 ± 0.02	3.5 ± 0.7	3.71 ± 0.06	This work
NdY/CsSe	Se	1.7 ± 0.2	2.44 ± 0.02	3.1 ± 0.5	3.52 ± 0.02	1.5 ± 0.4	3.80 ± 0.02	This work
c-RbSe	Se	1	2.468	3	3.338	4	3.65[c]	[24]
	Rb	$\cdots$	$\cdots$	3	3.338	3	3.620	[24]
ℓ-CsSe (450 °C)	Cs	~ 1	~ 2.37	~ 3	~ 3.46	~ 3	~ 3.79	[25]

[a]a refers to the anomalous scattering atom in the case of the zeolite data and to the reference atom for coordination information in the case of the crystal and liquid data.
[b]Total coordination numbers calculated assuming $C_3(A, \text{Se}) = 3C_3(\text{Se}, \text{Se})$ as in c-RbSe.
[c]Average distance of 3 Rb and 1 Se atoms.

The combined evidence of the AXS and Raman scattering results, taken in conjunction with the TEM characterization and color changes in the zeolite on loading, makes it clear that the elemental Se and RbSe and CsSe compounds are being incorporated in the zeolite with disordered structures remarkably similar to the disordered bulk phases, in spite of the fact that only 8–16 atoms are involved. Subsequent studies of the temperature dependence of the structure and dynamics will elucidate the nature of the phase of the clusters and reveal possible transitions between different phases.
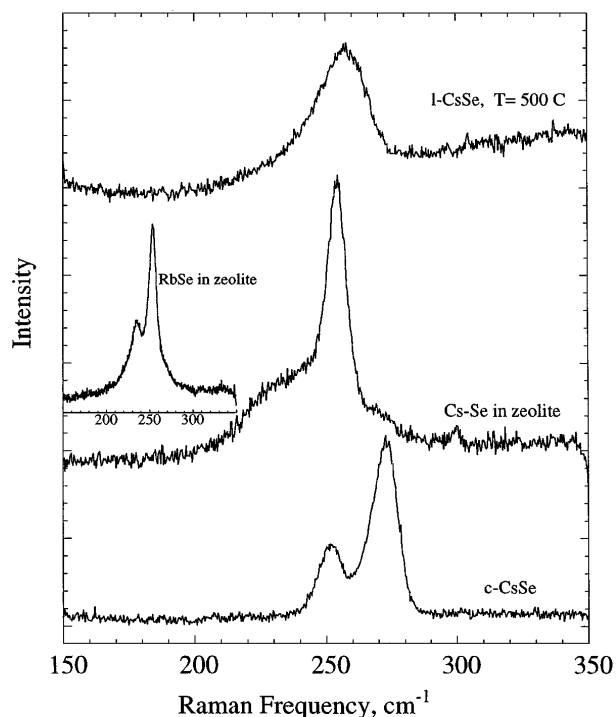
*Present address: Lab. de Physicochimie des Materiaux Solides, CNRS Montpellier, Pl. Eugène Bataillon C.C. 03, 34095 Montpellier, France.
†Present address: Fachbereich Phys. Chemie, Wilhelms Üniversität Münster, Münster, Germany.

[1] L. E. Brus, J. Phys. Chem. **90**, 2555 (1986).
[2] S. L. Lai *et al.,* Phys. Rev. Lett. **77**, 99 (1996).
[3] J. B. Parise *et al.,* Inorg. Chem. **27**, 221 (1988).
[4] H. Endo *et al.,* Jpn. J. Appl. Phys. **32**, 773 (1993); K. Tamura *et al.,* J. Phys. Soc. Jpn. **55**, 528 (1986).
[5] V. N. Bogomolov *et al.,* JETP Lett. **42**, 517 (1985).
[6] O. Terasaki *et al.,* Nature (London) **330**, 58 (1987).
[7] Y. Katayama, K. Maruyama, and H. Endo, J. Non-Cryst. Solids **117/118**, 485 (1990).
[8] T. Arai *et al.,* Surf. Rev. Lett. **3**, 707 (1996).
[9] G. Schulz-Ekloff, in *Zeolite Chemistry and Catalysis,* edited by P. A. Jacobs *et al.* (Elsevier, Amsterdam, 1991), p. 65.
[10] J. M. Thomas, Philos. Trans. R. Soc. London A **333**, 173 (1990).
[11] P. Armand, L. Iton, J. W. Richardson, and M.-L. Saboungi (private communication).
[12] D. L. Price *et al.,* Phys. Rev. B **55**, 11 249 (1997).
[13] P. Cherin and P. Unger, Inorg. Chem. **6**, 1589 (1967).
[14] O. Foss and V. Janickis, J. Chem. Soc. Dalton Trans. **1980**, 624 (1980).
[15] Y. Miyamoto, Jpn. J. Appl. Phys. **19**, 1813 (1980).
[16] R. W. Johnson *et al.,* J. Non-Cryst. Solids **83**, 251 (1986).
[17] M. Misawa and K. Suzuki, Trans. Jpn. Inst. Met. **18**, 427 (1977).
[18] M. Misawa and K. Suzuki, Trans. J. Phys. Soc. Jpn. **44**, 1612 (1978).
[19] Y. Nozue *et al.,* J. Phys. Condens. Matter **2**, 5209 (1990).
[20] P. J. Carroll and J. S. Lannin, J. Non-Cryst. Solids **35/36**, 1277 (1980).
[21] G. Lucovsky, in *The Physics of Selenium and Tellurium* (Springer, Berlin, 1979).
[22] See, for example, A. Goldbach, L. Iton, M. Grimsditch, and M.-L. Saboungi, J. Phys. Chem. **101**, 330–334 (1997).
[23] J. Fortner, M.-L. Saboungi, and J. E. Enderby, Phys. Rev. Lett. **69**, 1415 (1992).
[24] P. Boettcher, Angew. Chem. **27**, 759 (1988).
[25] M.-L. Saboungi, J. Fortner, L. A. Curtiss, and W. S. Howells (private communication).

FIG. 4. Depolarized Raman spectra of bulk c-CsSe, CsSe in Nd-Y zeolite, and bulk ℓ-CsSe. Inset: RbSe in Nd-Y zeolite.